Profile effect on the feasibility of extinction-based localized surface plasmon resonance biosensors with metallic nanowires

Kyung Min Byun, Sung June Kim, and Donghyun Kim

We investigate the effect of the cross-sectional profile of an array of metallic nanowires on the feasibility of a localized surface plasmon resonance (LSPR) biosensor. Calculations were performed using rigorous coupled-wave analysis with an emphasis on the extinction properties of the LSPR structure. The results indicate that the nanowire structure, particularly that of a T-profile, delivers an extremely linear sensing performance over a wide range of the target refractive index with much enhanced sensitivity. The extinction-based LSPR structure also involves a relatively large dimension and thus is expected to provide a feasible biosensor using current semiconductor technology. © 2006 Optical Society of America

OCIS codes: 050.2770, 130.6010, 240.6680.

1. Introduction

A surface plasmon resonance (SPR) biosensor is an optical device based on the excitation of surface plasmons, in which plasma oscillations in a metal film are excited by the incident light in the attenuated total reflection configuration to be used as a sensitivity indicator.[1–5] In the resonance condition, incident light energy is mostly absorbed as excited evanescent waves are coupled to binding analytes on a thin metal film. Since the reflectance curve exhibits a minimum at resonance, surface reactions of interest can be quantified by measuring the shift of the reflectance curve.

Surface plasmons can also be excited in metallic nanostructures. It is well known that noble-metal nanostructures allow direct and strong optical coupling of the incident light to resonantly driven electron plasma oscillations, called localized surface plasmons (LSPs).[6] Metallic nanostructures, if significantly smaller than the light wavelength, show an intense optical absorption band in the visible range.[7] Compared with surface plasmon polaritons (SPPs) excited in a thin metal film, the LSP resonance (LSPR) excitation is characteristic of substantial enhancement of electromagnetic fields as a result of strong absorption and highly efficient light scattering.[8] These enhanced fields induce significantly high sensitivity to changes in the local environment caused by binding molecules surrounding the nanostructures.[9,10]

For this reason, many researchers have proposed SPR biosensing systems incorporating metallic nanostructures for various sensing applications.[11–14] Typical experiments involve gold or silver nanostructures deposited over a thin metal film to bind with specific target analytes and to excite the localized plasmons. The experimental results indicated that these modified sensing schemes improve sensitivity more than ten times compared with a conventional SPR biosensor.[11,13] However, nanostructure-modified SPR biosensors have a fundamental constraint that SPP–LSP interactions can limit the effectiveness of excited LSP modes.[15]

Recently, regularly patterned metallic nanostructure arrays without a metal film on a dielectric substrate have drawn tremendous interest as a potential tool to implement biosensors.[16,17] This configuration is fully based on the LSP modes; thus its performance is not interfered by the SPP–LSP interactions. Unlike a biosensor based on SPP–LSP coupled modes, field enhancement is mostly associated with the coupling effects between resonant LSP modes that are excited in an ensemble of interacting nanostructures and is

K. M. Byun and S. J. Kim are with the School of Electrical Engineering and Computer Science, Seoul National University, Seoul, South Korea. D. Kim (kimd@yonsei.ac.kr) is with the School of Electrical and Electronic Engineering, Yonsei University, Seoul 120-749, South Korea.

Received 6 September 2005; revised 9 December 2005; accepted 12 December 2005; posted 14 December 2005 (Doc. ID 64627).

0003-6935/06/143382-08$15.00/0

© 2006 Optical Society of America

attributed to the sensitivity enhancement of a LSPR biosensor.[18–20] The specific nature of the field enhancement in a metallic nanostructure depends on intrinsic parameters, such as material, size, and shape, as well as extrinsic factors of the surrounding local media.[6,7,21] These LSPR devices can therefore serve as a transmission-based biosensor with extremely high sensitivity.[16] For example, it was shown that an extinction spectrum of the LSPR induced by silver nanoparticles is highly sensitive to the specific binding of antibiotin to a biotinylated surface.[22] It was also reported that regularly distributed triangular nanoparticles are more sensitive than spherical colloidal nanoparticles due to the shape dependence of the plasmon resonance and the coupling effect between nanoparticles, so that an ensemble of periodic silver nanoparticles can be applied to a nanoscale optical biosensor.

The resonant field enhancement from periodic metal arrays is far greater than that of aperiodic arrays or randomly roughened metal surfaces.[23] Thus the periodicity of an ensemble of nanostructures is an important parameter that needs to be considered. Suppose that we have well-separated and noninteracting nanostructures. According to the Mie-scattering theory, the optical extinction of interaction-free spherical metallic nanoparticles can be obtained as follows[6]:

$$E(\omega) = \frac{9\omega\varepsilon_m^{3/2}V}{c}\left\{\frac{\varepsilon_i(\omega)}{[\varepsilon_r(\omega)+2\varepsilon_m]^2+\varepsilon_i(\omega)^2}\right\}. \quad (1)$$

$E(\omega)$ is the optical extinction (i.e., sum of absorption and scattering), ω is the angular frequency of the exciting radiation, ε_m is the dielectric function of the binding layer on the nanostructure, V is the nanostructure volume, $\varepsilon_r(\omega)$ and $\varepsilon_i(\omega)$ are the real and imaginary parts of the dielectric function of the metallic nanostructure, and c is the light velocity in the free space. As presented in Eq. (1), the resonance condition of the LSP is satisfied when $\varepsilon_r(\omega) = -2\varepsilon_m$ and $\varepsilon_i(\omega)$ is small. On the other hand, for a nonspherical nanostructure with a noncircular cross section, the shape and the dielectric function of the nanostructure primarily affect and determine the optical extinction properties.

In contrast to noninteracting nanostructures, if the period is notably less than the wavelength of the incident light, electromagnetic coupling of individual nanostructures has a prominent influence on the resonance condition. In general, two distinct types of interaction effects may occur in relation to the period. In a considerably short distance, short-range interactions between neighboring nanostructures induce near-field coupling that creates highly sensitive plasmons confined to metal boundaries. However, when the period exceeds the range of near-field coupling, far-field interactions prevail among nanostructure arrays, as have been elucidated using a dipole–dipole interaction model.[24] While an individual metallic nanostructure gives rise to dipole fields, induced dipoles oscillate resonantly in the neighboring nanostructures, leading to the formation of LSPs and local field enhancement. Using far-field interactions, metallic nanostructures can also be exploited as optical waveguides.[25]

Despite stronger field enhancement, a near-field coupling configuration can suffer from worse sensing performance and more difficult implementation as a sensor, compared with a configuration based on far-field coupling. The near-field coupling generally shows complicated extinction spectra with multiple resonance peaks, which makes it difficult to detect the main resonance response to biological binding events linearly. In addition, the near-field coupling structure can be extremely sensitive to fabrication errors involved in realizing nanostructures with a small period of a complicated profile. Consequently, we consider interacting nanostructures in the range of far-field coupling.

The goal of this study is to use nanowires to implement nanostructures for the simplicity of modeling and reliable fabrication and furthermore to understand relevant design issues to achieve maximal sensitivity enhancement as well as highly linear detection in sensing performance. For this purpose, we explore the profile dependence of optical extinction properties of excited LSP modes by introducing nanowire geometries of a T and an inverse T-profile and the effect of other design parameters such as the nanowire period on the sensor performance. Although a previous study showed that extremely large field enhancement is possible with asymmetric nanowire profiles less than 50 nm in size,[26] such a structure is tremendously difficult to fabricate and to produce binding events on the sharp and slanted slope.

2. Numerical Methods

We consider one-dimensional metallic nanowire gratings on a dielectric substrate as presented in Fig. 1(a). Silver or gold nanowires that are periodic in the x axis are assumed to be aligned in the y axis. The nanowires with a complex dielectric function are regularly patterned on a glass substrate ($n_s = 1.515$). The nanowire period (Λ) is considered in the range of 250–400 nm such that far-field dipolar interactions dominate. We assume that TM-polarized light, the electric field of which oscillates in parallel to the nanowire grating vector, is normally incident. Note also that both silver and gold were considered as nanowire material. Optical constants of silver and gold were taken from Ref. 27.

To describe the optical response of metallic nanowires, extinction spectra were calculated by rigorous coupled-wave analysis (RCWA),[28,29] which has been successfully applied to explaining optical responses of nanostructures.[30,31] Our RCWA routine has been found to corroborate the experimental results of earlier studies using metallic nanostructures in the range of a few tens of nanometers in size,[32] offering an effective scheme to analyze optical properties of nanowires including extinction spectra.

Optical extinction is defined as $-\log(T)$, where T denotes transmittance as a function of the light wave-

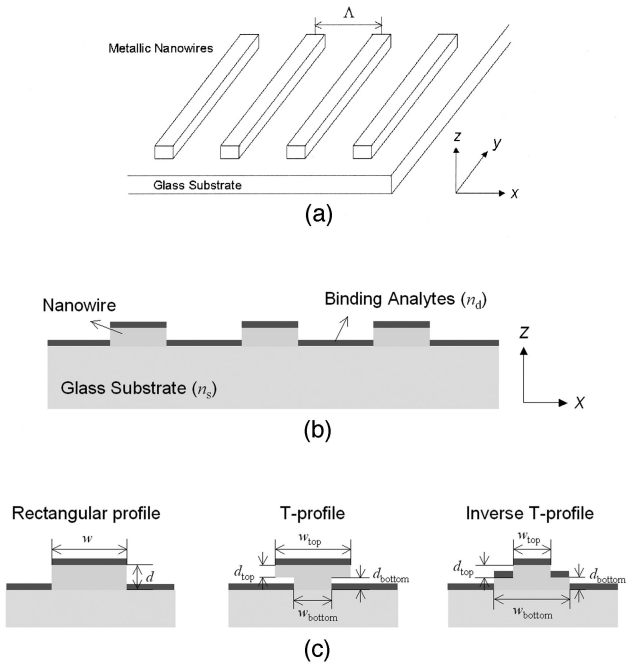

Fig. 1. (a) Schematic diagram of metallic nanowire arrays with a period Λ on a glass substrate. TM-polarized light is normally incident on a glass substrate. (b) Cross section of a nanowire-modified LSPR biosensor. Binding analytes are modeled as a 3 nm thick dielectric monolayer that covers both nanowires and a glass substrate. (c) Nanowire cross section of rectangular, T-, and inverse T-profiles. For a rectangle, $w = 100$ nm and $d = 20$ nm; for a T-profile, $w_{top} = 100$ nm, $w_{bottom} = 50$ nm, and $d_{top} = d_{bottom} = 10$ nm; for an inverse T-profile, $w_{top} = 50$ nm, $w_{bottom} = 100$ nm, and $d_{top} = d_{bottom} = 10$ nm.

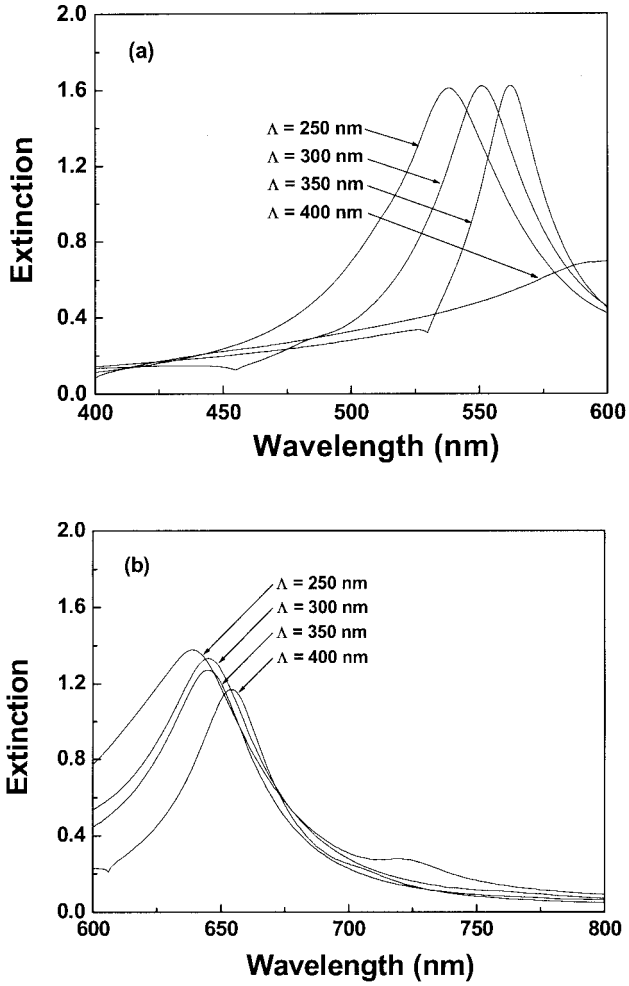

Fig. 2. Extinction spectra of nanowire arrays with a rectangular profile assuming no analytes. For (a) silver and (b) gold nanowires, $\lambda_{LSPR} = 562$ nm (silver) versus 645 nm (gold) at $\Lambda = 350$ nm. The peak extinction and its width (full width at half-maximum) are 1.623 and 36 nm (silver) versus 1.272 and 52 nm (gold).

length and is obtained from the diffraction efficiency of propagating orders that is calculated by coupled-wave equations, assuming that the light source is a unit-amplitude plane wave and that the permittivity in a metallic grating region can be written as a Fourier series expansion. The field inside the grating region is expanded in terms of space-harmonic components, which are phase matched to the diffraction orders.[28,29] By solving the wave equations, the field of each diffracted order outside the metallic grating is related to the corresponding space-harmonic field inside the grating volume.

To quantify the sensitivity of the LSPR sensing configuration with respect to changes in the refractive index of the dielectric media surrounding metallic nanowires, target binding between biomolecules is modeled with a dielectric monolayer. Here the refractive index change is induced by binding events of target analytes inside the flow channel and is assumed to represent the concentration change in binding events linearly. The thickness of this layer is assumed to be 3 nm based on the amplitude distribution of the excited plasmons that rapidly decreases outside the nanostructures. Note that the effect of LSP modes becomes insignificant if they are more than 3 nm away from the nanostructure surface for various cross sections.[26] As shown in Fig. 1(b), the monolayer covers the top surface of nanowires as well as the surface between nanowires on a glass substrate. The resonance wavelength shift is evaluated as the refractive index of the binding dielectric layer (n_d) increases from 1.0 to 1.5.

In our numerical model of one-dimensional metallic nanowires, we consider three different nanowire profiles: a rectangle, a T, or an inverse T as shown in Fig. 1(c), where w_{top} (w_{bottom}) denoting the width of the nanowire top (bottom) is either 100 or 50 nm. The nanowire depth d ($=d_{top} + d_{bottom}$) is fixed at 20 nm. A rectangular profile has the same width (=100 nm) of the nanowire top and bottom. In other words, $w_{top} = 100$ nm, $w_{bottom} = 50$ nm, and $d_{top} = d_{bottom} = 10$ nm for a T-profile and $w_{top} = 50$ nm, $w_{bottom} = 50$ nm, and $d_{top} = d_{bottom} = 10$ nm for an inverse T-profile. Consequently, T- and inverse T-profile nanowires take an equal volume if the period is identical.

3. Results and Discussion

In Figs. 2(a) and 2(b) extinction properties have been

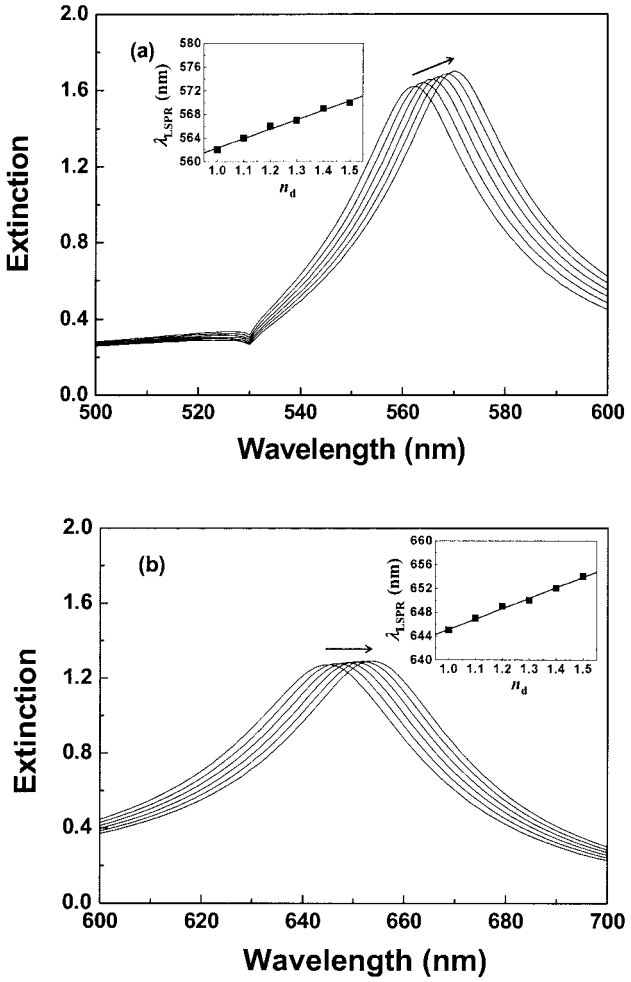

Fig. 3. Extinction spectra of rectangular nanowires of (a) silver and (b) gold at $\Lambda = 350$ nm as n_d increases from 1.0 to 1.5 (increase is in the direction of the arrow). The inset shows linear regression analysis between n_d and λ_{LSPR}.

calculated by various periods of Λ for silver and gold nanowire gratings, respectively, with a rectangular profile at $w = 100$ nm and $d = 20$ nm. The resonance wavelength (λ_{LSPR}) and the width of the extinction peak represent the LSPR and the damping of LSPs, respectively. λ_{LSPR} blueshifts (i.e., shifts toward a shorter wavelength) for both silver and gold nanowires as Λ is decreased from 400 to 250 nm. This is in good agreement with an empirical report for orderly patterned nanostructure arrays at a period that is approximately half the λ_{LSPR}.[19] At nanowire periods in the range of 200–500 nm, radiative dipole interactions between nanowires as well as large retardation effects are deemed responsible for the blueshift.

Obviously, the dielectric function of a metallic nanostructure has a dominant effect on the resonance condition. The difference in the dielectric function causes λ_{LSPR} of gold nanowires to be located at longer wavelengths than that of silver. More specifically, because the imaginary part of the dielectric function of gold is larger than that of silver, the extinction of gold nanowires generally has a lower maximum value at resonance, which can be deduced from Eq. (1).

For both silver and gold nanowires, the nanowire period for optimal biosensing was determined to be 350 nm since it provides relatively large extinction and narrow resonance width [full width at half-maximum (FWHM)] than at other periods. In Fig. 2(b), even though the extinction spectrum at $\Lambda = 250$ nm exhibits larger extinction, its resonance width is larger, which indicates poorer selectivity in sensing applications. As a result, $\Lambda = 350$ nm is employed for silver and gold nanowires in what follows, unless noted otherwise, in calculating the shift of λ_{LSPR} with the refractive index. As will be clear, the optimum period $\Lambda = 350$ nm is also valid for a T- and an inverse T-profile as well as a rectangular profile.

Note that the grating effect due to the excitation of higher-order diffraction can affect the extinction properties of LSPR structures. If Λ is such that the first diffraction order is radiative for the whole spectral range, the grating effect can be ignored.[33] In other words, when $\Lambda > \lambda_{max}/n_s$ (λ_{max} is the longest wavelength in extinction spectra and n_s is a refractive index of the dielectric substrate), at which the transition between evanescent and radiative modes occurs, no coupling of individual nanostructures is found, so that the structure can be regarded as an isolated single structure. For far-field interactions, however, the transition of the first diffraction order from an evanescent to a radiative mode is observed to have a prominent effect on the plasmon damping and therefore on the spectral width of the plasmon extinction peak.[33] In short, the first diffraction order radiates into the substrate for wavelengths $\lambda_{rad} < n_s\Lambda$, whereby the increased radiation damping leads to an increase of the extinction spectral width.

In Fig. 3(a) the transition between evanescent and radiative modes appears at $\lambda = 530.3$ nm in the calculated extinction spectra. The grating effect, however, is not significant as the transition wavelength is far off from the resonance wavelength λ_{LSPR} for both nanowire materials. The transition due to the grating effect also appears with gold nanowires at $\lambda = 530.3$ nm, which is not in the range shown in Fig. 3(b).

As the refractive index of a dielectric binding layer increases from 1.0 to 1.5, λ_{LSPR} shifts to a longer wavelength (redshift). For a rectangular profile, total spectral changes are 8 nm for silver nanowires and 9 nm for gold, as respectively shown in the insets of Figs. 3(a) and 3(b). Linear regression analyses show that the shift is fairly linear over the whole range of refractive indices and that the refractive index sensitivities are 16.0 nm/RIU for silver and 17.4 nm/RIU for gold (RIU stands for refractive index unit). R is the correlation coefficient that denotes the linearity obtainable in the sensor performance. R^2 values for silver and gold nanowires of a rectangular profile are 0.994 and 0.997, respectively.

In what follows, the effect of the nanowire profile on the sensitivity is estimated by comparing two

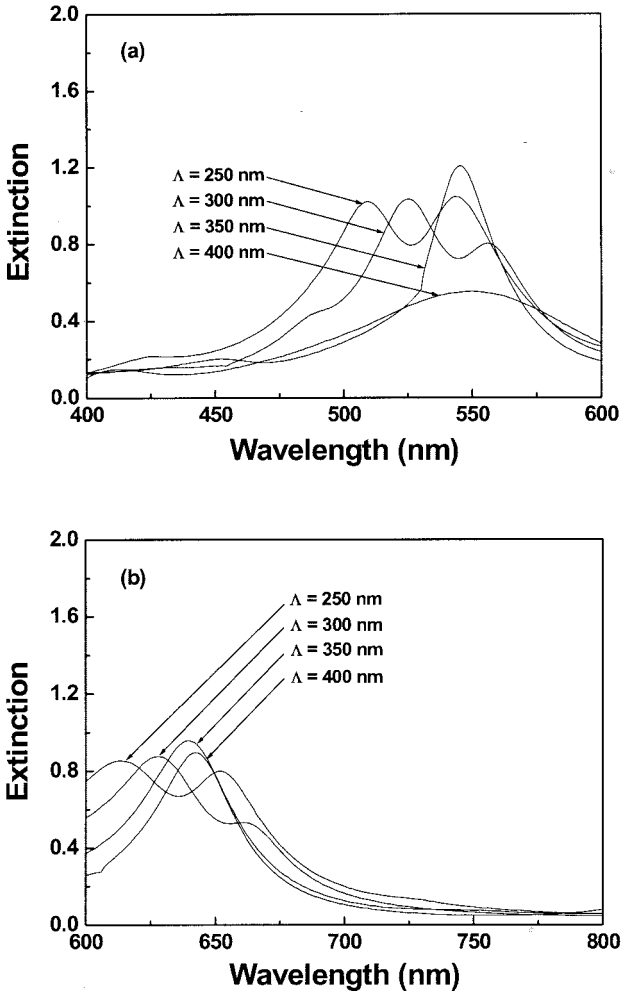

Fig. 4. Extinction spectra of nanowire arrays with a T-profile assuming no analytes. For (a) silver and (b) gold nanowires, λ_{LSPR} = 546 nm (silver) versus 640 nm (gold) at Λ = 350 nm. The peak extinction and its width (FWHM) are 1.206 and 33 nm (silver) versus 0.957 and 49 nm (gold).

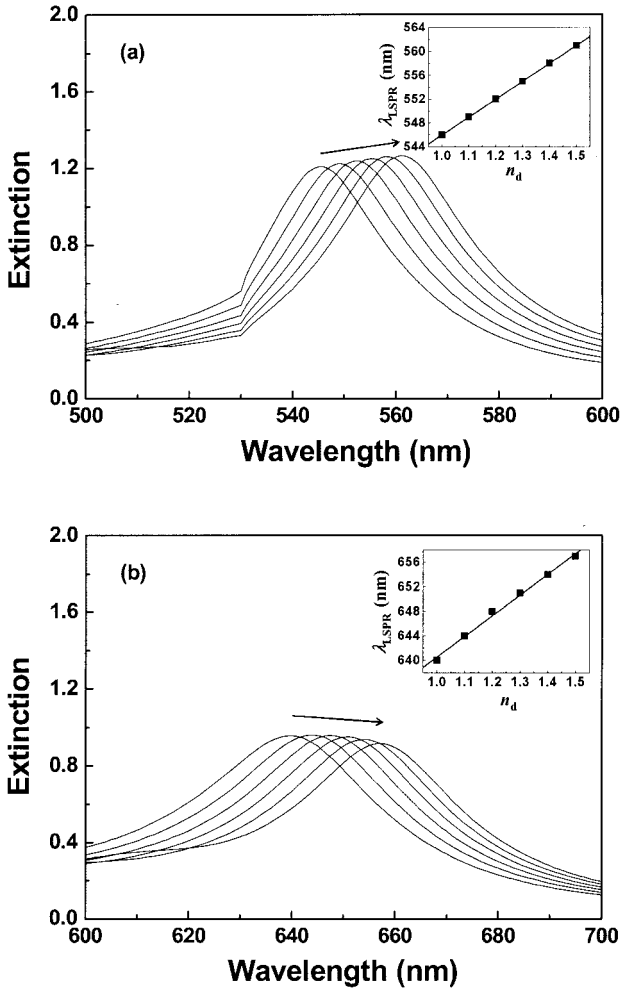

Fig. 5. Extinction spectra of (a) silver and (b) gold nanowires of a T-profile at Λ = 350 nm as n_d increases from 1.0 to 1.5 (increase is in the direction of the arrow). The inset shows linear regression analysis between n_d and λ_{LSPR}.

different nanowire profiles, a T- and an inverse T-profile, with a rectangular profile. Figure 4 shows the extinction spectra at various periods (Λ = 250–400 nm) of silver and gold nanowires for a T-profile. Similar to the results of a rectangular profile in Fig. 2, the extinction spectra still have maximum values at λ = 500–600 nm for silver and λ = 600–700 nm for gold. In particular, at Λ = 250 and 300 nm, both silver and gold nanowires of a T-profile show multiple extinction peaks. These additional extinction peaks originate from the excitation of higher-order harmonics of multipolar plasmon oscillations, induced by the complex nanowire profile. Since the optical near-field distribution around a nanostructure is affected by the order of excited multipolar plasmon modes, which modify optical properties of metallic nanowires intricately,[34] the extinction spectra also present a less linear sensitivity characteristic to binding biomolecular changes.

The extinction effects of the T-profile on the refractive-index sensitivity are shown in Fig. 5, which represents extinction spectra and the change of an extinction peak with n_d. For silver nanowires, the resonance shift to an increase of n_d is completely linear with a sensitivity equal to 30 nm/RIU. This is almost two times larger than in the case of a rectangular profile. Gold nanowires of a T-profile also exhibit improved sensitivity of 33.7 nm/RIU compared with rectangular gold nanowires at an identical period (Λ = 350 nm) as depicted in the inset of Fig. 5.

Second, an inverse T-profile has been calculated at various periods (Λ = 250–400 nm). The results are shown in Fig. 6 for silver and gold nanowires. The difference in the dielectric function between silver and gold leads to a larger extinction maximum and shorter resonance wavelength with silver than in the case of gold. Moreover, in extinction spectra at Λ = 250 and 300 nm, similar to a T-profile, secondary peaks originating from multipolar plasmon modes appear in the wavelength range $\lambda < \lambda_{LSPR}$ for both silver and gold nanowires. At this period, the refractive index sensitivity cannot be identified as linear, as the higher-order terms significantly influence the op-

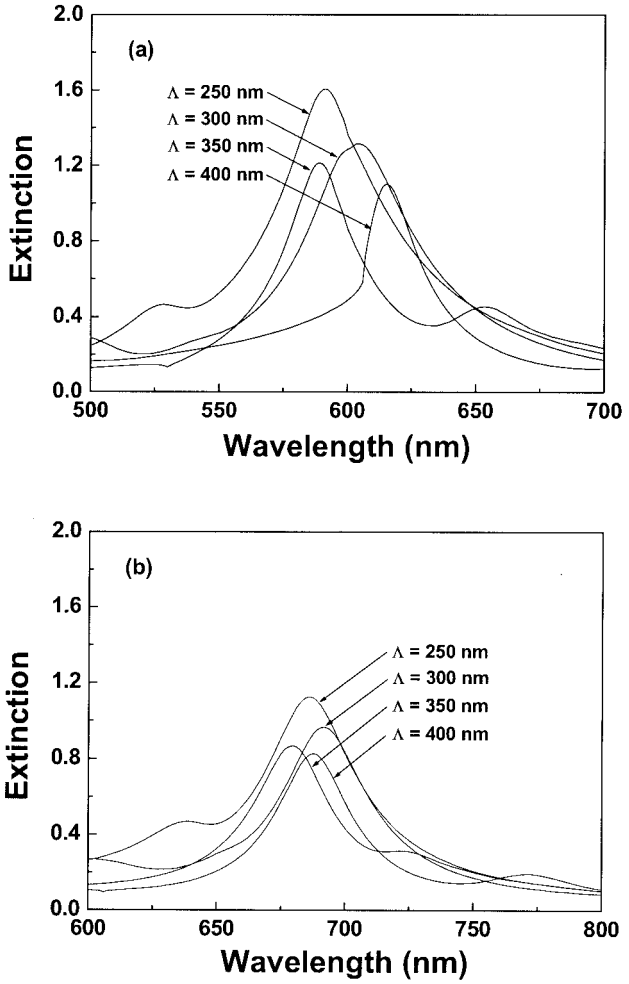

Fig. 6. Extinction spectra of nanowire arrays with an inverse T-profile assuming no analytes. For (a) silver and (b) gold nanowires, $\lambda_{LSPR} = 589$ nm (silver) versus 679 nm (gold) at $\Lambda = 350$ nm. The peak extinction and its width (FWHM) are 1.214 and 38 nm (silver) versus 0.868 and 42 nm (gold).

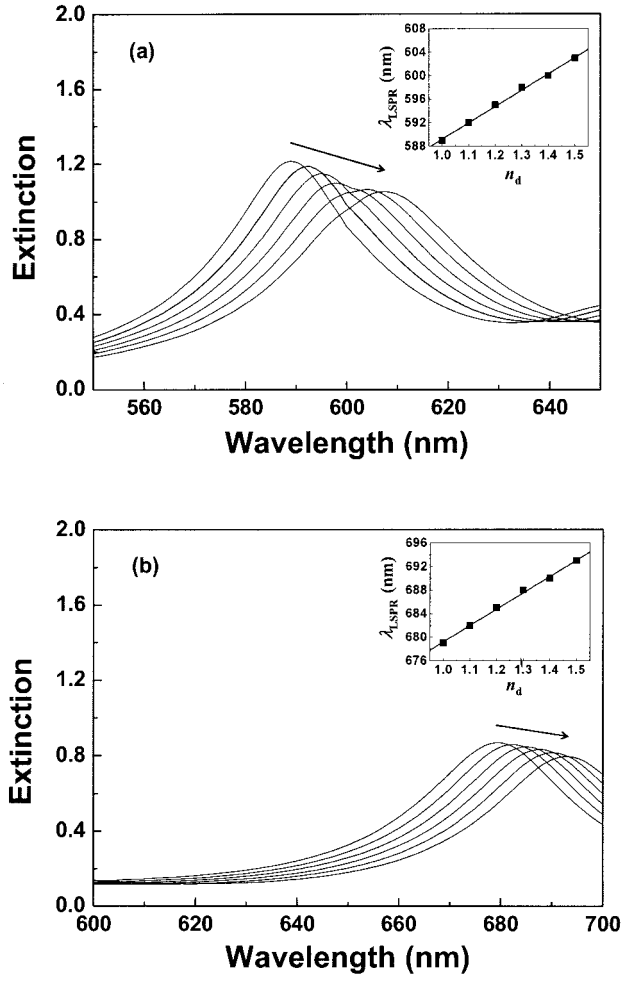

Fig. 7. Extinction spectra of (a) silver and (b) gold nanowires of an inverse T-profile at $\Lambda = 350$ nm as n_d increases from 1.0 to 1.5 (increase is in the direction of the arrow). The inset shows linear regression analysis between n_d and λ_{LSPR}.

tical performance of a LSPR biosensor. Sensitivity improvement is also observed at $\Lambda = 350$ nm for an inverse T-profile. In Fig. 7, λ_{LSPR} shows a redshift as n_d increases with the sensitivity of 27.7 nm/RIU for both silver and gold nanowires, a largely enhanced value compared with that of a rectangular profile.

As listed in Table 1, it is apparent that the nanowire profile affects the LSPR sensor performance, the sensitivity in particular, tremendously. For instance, the field inside a circular nanostructure, which is highly symmetric, becomes almost homogeneous and the field amplitude decays drastically outside the nanostructure.[26] It was also found that the field is highly heterogeneous for nonrectangular profiles and that especially at main resonance with a maximum extinction value the field amplitude takes large values at corners. In other words, the field amplitude is enhanced rapidly as the profile of a nanostructure becomes more complex and asymmetric.

This plasmonic interpretation based on the corner effect and the field enhancement for a nonrectangular profile can be applied to analyzing our results. As a T- or an inverse T-profile mimics a trapezoid that is an intermediate state between a rectangle and a triangle, the two profiles present larger field amplitude enhancement with more strongly excited LSPs and induce higher sensitivity, associated with less symmetry than a rectangular profile. Furthermore, the two profiles provide a more feasible structure with enhanced customizability than a triangular or an inverse triangular profile.

In our results, a T-profile on the whole shows better sensitivity to the change of refractive indices than an inverse T-profile. To qualitatively understand the difference in the performance of the two profiles, suppose we approximate a T-profile as an inverted trapezoid and an inverse T-profile as a trapezoid, respectively, such that they occupy an equal volume. The corner effect stipulates that when the resonance occurs, extremely strong fields are excited in the vicinity of corners in nanostructures. For an inverted trapezoid, fields are enhanced mainly at two vertices on the top, where the binding events of target ana-

Table 1. Calculated Sensitivity (in nm/RIU) and Squared Correlation Coefficient (R^2) for Silver and Gold Nanowires of Different Profiles at Λ = 350 nm

Profile	Silver	Gold
Sensitivity		
Rectangular	16.0	17.4
T	30.0	33.7
Inverse T	27.7	27.7
Squared Correlation Coefficient		
Rectangular	0.994	0.997
T	1.000	0.997
Inverse T	0.998	0.998

Table 2. FWHM of Extinction Spectra (in nm) Calculated for Silver and Gold Nanowires of Different Profiles at Λ = 350 nm

Profile	Silver	Gold
Rectangular	36.7	50.5
T	36.0	46.3
Inverse T	40.8	42.0

lytes occur. In contrast, the field enhancement for a trapezoid structure occurs at both end points on the bottom, which is relatively far from the layer of target analytes. In consequence, a closer distance between highly enhanced fields and the binding events results in better sensitivity performance for nanowires of a T-profile.

The resonance width is another important measure of the SPR-based sensor performance. Table 2 shows the FWHM of the extinction spectra calculated for silver and gold nanowires of different profiles at Λ = 350 nm. In terms of FWHM, silver nanowires generally show a sharper resonance curve and perform better selectivity than gold. Overall data based on the sensitivity and FWHM shown in Tables 1 and 2 indicate that silver nanowires of a T-profile exhibit optimum characteristics.

So far, the effects of the nanowire profile on the extinction spectrum and the sensing performances have been investigated. Consider now the effect of the dielectric function of metallic nanostructures briefly. As mentioned earlier, the dielectric function of the nanowire material significantly affects the extinction characteristics. Since the real part determines the resonance wavelength, λ_{LSPR} for silver nanowires is found at a shorter wavelength than that of gold nanowires in all nanowire profiles. On the other hand, the imaginary parts are related to the damping of excited LSPs; thus the extinction spectra of gold nanowires show smaller amplitude at the resonance wavelength and larger resonance width than silver.

Actual fabrication of nanowires of T- or inverse T-profiles examined in this paper can be performed using electron-beam or interference lithography with a laser in the visible wavelength. This study suggests a periodic structure with Λ = 350 nm, which can also be implemented with deep-UV lithography.

4. Conclusion

In this study we have calculated optical extinction properties of silver and gold nanowires on a dielectric substrate using RCWA. Our results show that the resonance spectrum strongly depends on the nanowire period and profile. For nanowire periods in the far-field coupling, dipole interactions between metallic nanowires result in a blueshift of λ_{LSPR} as Λ varies from 400 to 250 nm. The complexity of the LSPR extinction spectrum has been discussed for silver and gold nanowires with a T- and an inverse T-profile.

Our results indicate that the extinction spectra of the LSPR sensor based on metallic nanowires are fairly linear and significantly sensitive to changes of refractive indices of dielectric binding media if design parameters are properly optimized. In our investigation, Λ = 350 nm achieves both high extinction peak and narrow resonance width for the profiles considered. For both silver and gold nanowires, the T- and the inverse T-profiles exhibit better sensitivity than a rectangular profile. In particular, a T-profile presents the highest sensitivity of 33.7 nm/RIU for gold and 30.0 nm/RIU for silver. Also, for a T-profile, silver nanowires exhibit narrower resonance width than gold. This study is expected to provide a basis to implement feasible structures as a LSPR biosensor based on metallic nanowires with excellent sensing performance.

This work was supported by the Science Research Center and Engineering Research Center program of the Ministry of Science and Technology of the Korea Science and Engineering Foundation (KOSEF) (R11-2000-075-01001-1). D. Kim acknowledges the support by KOSEF through the National Core Research Center for Nanomedical Technology (R15-2004-024-00000-0) and by the Korea Research Foundation Grant funded by the Korean government (MOEHRD) under KRF-2005-205-D00051.

References

1. H. Raether, *Surface Plasmons on Smooth and Rough Surfaces and on Gratings* (Springer-Verlag, 1988).
2. B. Liedberg, C. Nylanderm, and I. Lundström, "Surface plasmon resonance for gas detection and biosensing," Sens. Actuators **4,** 299–304 (1983).
3. K. Matsubara, S. Kawata, and S. Minami, "Optical chemical sensor based on surface plasmon measurement," Appl. Opt. **27,** 1160–1163 (1988).
4. J. Homola, S. S. Yee, and G. Gauglitz, "Surface plasmon resonance sensors: review," Sens. Actuators B **54,** 3–15 (1999).
5. M. J. O'Brien II, V. H. Pérez-Luna, S. R. J. Brueck, and G. P. López, "A surface plasmon resonance array biosensor based on spectroscopic imaging," Biosens. Bioelectron. **16,** 97–108 (2001).
6. U. Kreibig and M. Vollmer, *Optical Properties of Metal Clusters* (Springer-Verlag, 1995).
7. P. Mulvaney, "Surface plasmon spectroscopy of nanosized metal particles," Langmuir **12,** 788–800 (1996).
8. T. R. Jensen, M. D. Malinsky, C. L. Haynes, and R. P. Van Duyne, "Nanosphere lithography: tunable localized surface plasmon resonance spectra of silver nanoparticles," J. Phys. Chem. B **104,** 10549–10556 (2000).
9. T. Okamoto, I. Yamaguchi, and T. Kobayashi, "Local plasmon sensor with gold colloid monolayers deposited upon glass substrates," Opt. Lett. **25,** 372–374 (2000).

10. G. Kalyuzhny, M. A. Schneeweiss, A. Shanzer, A. Vaskevich, and I. Rubinstein, "Differential plasmon spectroscopy as a tool for monitoring molecular binding to ultrathin gold films," J. Am. Chem. Soc. **123,** 3177–3178 (2001).
11. L. A. Lyon, D. J. Pena, and M. J. Natan, "Surface plasmon resonance of Au colloid-modified Au films: particle size dependence," J. Phys. Chem. B **103,** 5826–5831 (1999).
12. E. Hutter, S. Cha, J.-F. Liu, J. Park, J. Yi, J. H. Fendler, and D. Roy, "Role of substrate metal in gold nanoparticle enhanced surface plasmon resonance imaging," J. Phys. Chem. B. **105,** 8–12 (2001).
13. L. He, M. D. Musick, S. R. Nicewamer, F. G. Salinas, S. J. Benkovic, M. J. Natan, and C. D. Keating, "Colloidal Au-enhanced surface plasmon resonance for ultrasensitive detection of DNA hybridization," J. Am. Chem. Soc. **122,** 9071–9077 (2000).
14. K. M. Byun, S. J. Kim, and D. Kim, "Design study of highly sensitive nanowire-enhanced surface plasmon resonance biosensors using rigorous coupled wave analysis," Opt. Express **13,** 3737–3742 (2005).
15. T. Kume, N. Nakagawa, S. Hayashi, and K. Yamamoto, "Interaction between localized and propagating surface plasmons: Ag fine particles on Al surface," Solid State Commun. **93,** 171–175 (1995).
16. A. D. McFarland and R. P. Van Duyne, "Single silver nanoparticles as real-time optical sensors with zeptomole sensitivity," Nano Lett. **3,** 1057–1062 (2003).
17. J. J. Mock, D. R. Smith, and S. Schultz, "Local refractive index dependence of plasmon resonance spectra from individual nanoparticles," Nano Lett. **3,** 485–491 (2003).
18. E. Hutter and J. H. Fendler, "Exploitation of localized surface plasmon resonance," Adv. Mater. **16,** 1685–1706 (2004).
19. C. L. Haynes, A. D. McFarland, L. Zhao, R. P. Van Duyne, G. C. Schatz, L. Gunnarsson, J. Prikulis, B. Kasemo, and M. Käll, "Nanoparticle optics: the importance of radiative dipole coupling in two-dimensional nanoparticle arrays," J. Phys. Chem. B **107,** 7337–7342 (2003).
20. S. Enoch, R. Quidant, and G. Badenes, "Optical sensing based on plasmon coupling in nanoparticle arrays," Opt. Express **12,** 3422–3427 (2004).
21. C. Sönnichsen, T. Franzl, T. Wilk, G. von Plessen, J. Feldmann, O. Wilson, and P. Mulvaney, "Drastic reduction of plasmon damping in gold nanorods," Phys. Rev. Lett. **88,** 077402 (2002).
22. A. J. Haes and R. P. Van Duyne, "A nanoscale optical biosensor: sensitivity and selectivity of an approach based on the localized surface plasmon resonance spectroscopy of triangular silver nanoparticles," J. Am. Chem. Soc. **124,** 10596–10604 (2002).
23. D. A. Genov, A. K. Sarychev, V. M. Shalaev, and A. Wei, "Resonant field enhancements from metal nanoparticle arrays," Nano Lett. **4,** 153–158 (2004).
24. W. Rechberger, A. Hohenau, A. Leitner, J. R. Krenn, B. Lamprecht, and F. R. Aussenegg, "Optical properties of two interacting gold nanoparticles," Opt. Commun. **220,** 137–141 (2003).
25. S. A. Maier, M. L. Brongersma, P. G. Kik, S. Meltzer, A. A. G. Requicha, and H. A. Atwater, "Plasmonics—a route to nanoscale optical devices," Adv. Mater. **13,** 1501–1505 (2001).
26. J. P. Kottmann, O. J. F. Martin, D. R. Smith, and S. Schultz, "Plasmon resonances of silver nanowires with a nonregular cross section," Phys. Rev. B **64,** 235402 (2001).
27. E. D. Palik, *Handbook of Optical Constants of Solids* (Academic, 1985).
28. M. G. Moharam and T. K. Gaylord, "Diffraction analysis of dielectric surface-relief gratings," J. Opt. Soc. Am. **72,** 1385–1392 (1982).
29. M. G. Moharam and T. K. Gaylord, "Rigorous coupled-wave analysis of metallic surface-relief gratings," J. Opt. Soc. Am. A **3,** 1780–1787 (1986).
30. J. Lermé, "Introduction of quantum finite-size effects in the Mie's theory for a multilayered metal sphere in the dipolar approximation: application to free and matrix-embedded noble metal clusters," Eur. Phys. J. D **10,** 265–277 (2000).
31. E. Moreno, D. Emi, C. Hafner, and R. Vahldieck, "Multiple multipole method with automatic multipole setting applied to the simulation of surface plasmons in metallic nanostructures," J. Opt. Soc. Am. A **19,** 101–111 (2002).
32. K. M. Byun, D. Kim, and S. J. Kim, "Investigation of the sensitivity enhancement of nanoparticle-based surface plasmon resonance biosensors using rigorous coupled-wave analysis," in *Plasmonics in Biology and Medicine II,* T. Vo-Dinh, J. R. Lakowicz, and Z. K. Gryczynski, eds., Proc SPIE **5703,** 61–70 (2005).
33. G. Schider, J. R. Krenn, W. Gotschy, B. Lamprecht, H. Ditlbacher, A. Leitner, and F. R. Aussenegg, "Optical properties of Ag and Au nanowire gratings," J. Appl. Phys. **90,** 3825–3830 (2001).
34. J. R. Krenn, G. Schider, W. Rechberger, B. Lamprecht, A. Leiter, F. R. Aussenegg, and J. C. Weeber, "Design of multipolar plasmon excitations in silver nanoparticles," Appl. Phys. Lett. **77,** 3379–3381 (2000).